Stress on the Mediterranean Outflow Plume: Part II. Turbulent Dissipation and Shear Measurements

GREGORY C. JOHNSON

Applied Physics Laboratory, University of Washington, Seattle, Washington

ROLF G. LUECK

School of Earth and Ocean Sciences, University of Victoria, Victoria, British Columbia, Canada

THOMAS B. SANFORD

Applied Physics Laboratory and School of Oceanography, University of Washington, Seattle, Washington

(Manuscript received 4 March 1993, in final form 11 January 1994)

ABSTRACT

Bottom and interfacial stresses on the Mediterranean outflow plume are estimated using vertical profiles of turbulent dissipation and velocity collected in the Gulf of Cadiz. Turbulent dissipation is high throughout the plume, with a local minimum often present near the plume nose (depth of maximum downstream velocity). Bottom stresses are estimated by applying a log-layer model to the dissipation measurements. The dissipation measurements are also divided by plume-scale vertical shear from the horizontal velocity profiles to construct profiles of stress within the plume. The mean stress estimates in the bottom layer agree well with those calculated in the log layer from the dissipation measurements alone. The bottom-layer means are slightly larger than those of the interfacial layer. The maximum stresses in each layer are uncertain, since they depend on the ill-defined shape of the stress profiles within the plume. Dissipation-derived stress estimates in the log layer and those from dissipation measurements combined with the plume-scale vertical shear of horizontal velocity are roughly one-third the magnitude of those made in the log layer from velocity measurements and those made in the interfacial layer from the residuals of bulk mass and volume budgets (Part I). Possible reasons for this discrepancy are advanced.

1. Introduction

The Mediterranean outflow plume is a warm, salty, dense current that originates in the Mediterranean Sea, flows west through the Strait of Gibraltar, mixes with ambient water above it, and slowly descends the continental slope as it flows rapidly to the northwest in the Gulf of Cadiz, reaching its equilibrium depth of about 1200 m as it enters the Atlantic Ocean. In the Gulf of Cadiz, the dynamics of this plume are complex, with bottom stress, interfacial stress, mixing, topography, and earth's rotation all contributing to the plume's evolution in varying proportions within the first 100 km of its origin (Price et al. 1993). A companion study (Johnson et al. 1994, hereafter JSB) discusses the vertical structure of water mass properties and velocity within the Mediterranean outflow plume. In JSB, bottom stresses are estimated by applying the velocity data to a log-layer model, and bulk interfacial and total stresses are estimated using velocity and density data.

Here, a log-layer model is used to calculate bottom stresses on the plume from turbulent dissipation profiles. These bottom stresses are a third the magnitude of those estimated from velocity profile data applied to the log-layer model by JSB. The turbulent dissipation profiles are also paired with nearly concurrent profiles of plume-scale vertical shear from profiles of horizontal velocity to yield profiles of stress throughout the plume bottom and interfacial layers. The means of these stresses in the bottom layer are similar in magnitude to those obtained from dissipation alone in the log layer. The mean stresses in the interfacial layer are slightly less than half those in the bottom layer. In both layers, the local estimates of stress on the plume are again significantly smaller than those from velocity and density data (JSB; Baringer 1993). Possible reasons for these discrepancies are discussed.

2. Data

The Gulf of Cadiz Experiment carried out in September 1988 included a CTD survey and extensive use

Corresponding author address: Dr. Gregory C. Johnson, NOAA/Pacific Marine Environmental Laboratory, 7600 Sand Point Way N.E. Bldg. 3, Seattle, WA 98115-0700.

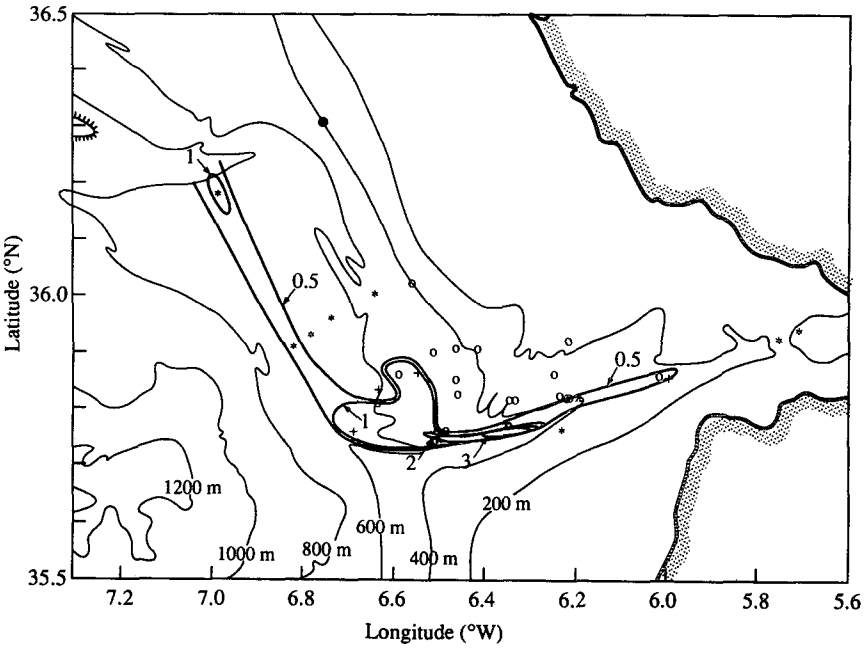

FIG. 1. Location of the 39 XDP drops with bottom stress contoured in pascals. There were 23 drops of matched XDP–XCP pairs with both XDP and XCP bottom stresses (open circles). There were five drops with no XCP bottom stress estimates (crosses). There were two drops of matched pairs with no XDP bottom stress estimates (multiply signs). There was one drop with both bottom stress estimates but no stress profiles (solid circle). There were eight drops with only XDP bottom stresses (asterisks). Bathymetry from Heezen and Johnson (1969) is contoured at 200-m intervals.

of expendable probes (Kennelly et al. 1989a). We use data from 54 expendable current profiler (XCP; Sanford et al. 1982) drops within the outflow plume (Kennelly et al. 1989b). To make estimates of turbulent dissipation, 61 expendable dissipation profilers (XDPs) were dropped, usually separated by about 2 minutes and at least 200 meters from the corresponding XCP drop (Lynch and Lueck 1989). The XDPs measure vertical profiles of temperature and one component of vertical shear of horizontal velocity over wavenumbers of 3–120 cpm.

The XCPs yield vertical profiles of velocity and temperature with data points at roughly 0.28-m intervals to within 0.56 ± 0.14 m of the bottom. The reference velocities are unknown, but this is not important here because only the estimates of the vertical shear of horizontal velocity are used. The probe fall rate is corrected by comparing bandpassed vertical XCP temperature profiles with those from CTD stations occupied just prior to nearly all the drops (Prater 1991).

The XDPs are of two types. One is a standard design that collects data to depths of 500 m, falling at a rate of roughly 2.8 m s^{-1}. These probes provide high quality data, with background noise levels of turbulent dissipation of about 1×10^{-6} W m^{-3}. The other type is modified to reach depths of 1500 m, falling at a rate of roughly 1.8 m s^{-1}. These probes have background noise levels about ten times those of the conventional models, but this is not a problem for plume measurements because the level of turbulent dissipation is usually 1×10^{-3} to 1×10^{-1} W m^{-3}. A number of the modified probes yielded noisier data that are not used here.

Of the 61 XDP drops made during the entire experiment, 39 yielded good data in the region studied (all symbols; Fig. 1). For the log-layer stress estimates the turbulent dissipation is estimated over 0.1-m bins, with the bottom bin centered at 0.10 ± 0.05 m of the bottom. Of the 39 drops, 37 yielded good bottom stress estimates (all symbols but the multiply signs; Fig. 1), and 24 of these were paired with a velocity profile from which bottom stress could be estimated (open circles and the solid circle; Fig. 1). For the stress profiles, 1-s bins (about 2–3 m depending on probe type) are used to make turbulent dissipation estimates. Of the 30 good XCP–XDP pairs within the plume, 28 of the XDPs reached the bottom (open circles and crosses; Fig. 1). The other two nearly reached the bottom (multiply signs; Fig. 1). Most of the profiles used in both analyses are concentrated in the eastern part of the survey region.

3. Stress within the plume

Two different methods are used here to estimate the stresses on the plume. One method uses the turbulent

dissipation data in a log-layer model to estimate local friction velocities in the bottom boundary layer. These friction velocities are then used to calculate local estimates of bottom stress. The other method estimates stress throughout the plume using pairs of XCPs and XDPs. XDP dissipation profiles are divided by XCP profiles of the plume-scale vertical shear of horizontal velocity to yield profiles of stress within the plume. This second method is not entirely independent from the first, since both use the dissipation data. Nonetheless, the second method is tested by comparing mean stresses in the bottom layer of the plume with those from the log-layer method.

The vertical structure of turbulent dissipation within the plume is related to the vertical structure of velocity and water mass properties. The sharp nose of the velocity maximum in the plume is formed by the intersection of a bottom layer and an interfacial layer (JSB). Each layer is influenced by stress and vigorous mixing. The turbulent dissipation estimates support the assertion that mixing rates and stress values are high throughout nearly all of the plume (Fig. 2). Below the surface layer, turbulent dissipation values in the North Atlantic Central Water (NACW) above the plume are mostly below the probe noise levels of 10^{-6} W m^{-3}. Within the plume, turbulent dissipation reaches 10^{-3} to 10^{-2} W m^{-3} from the plume top (350-m depth for the profile shown) to the bottom (500 m). The plume-scale vertical shear of horizontal velocity has a minimum at the nose (Fig. 3), coincident with a local minimum in turbulent dissipation (430 m in Fig. 2). A

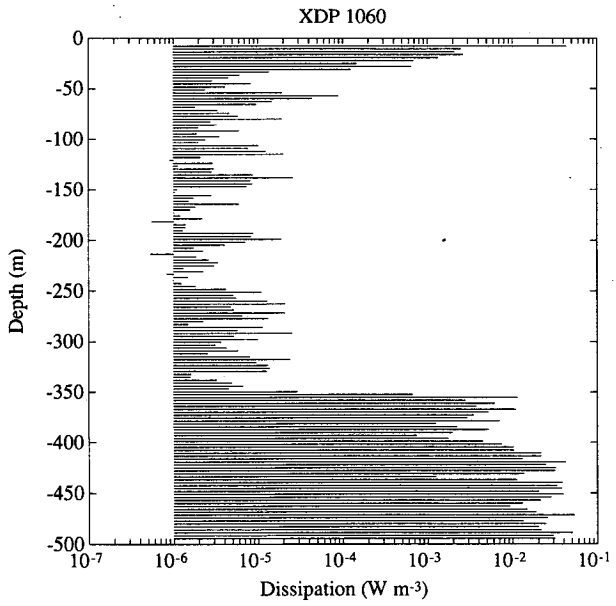

FIG. 2. Turbulent dissipation estimates from XDP 1060 at site 5 (Fig. 1 of JSB). The noise level of this instrument is slightly above 1×10^{-6} W m^{-3}. Turbulent dissipation is high from 350 m to the bottom, the extent of the plume. Turbulent dissipation has a slight local minimum near the plume nose around 430 m (see Fig. 3).

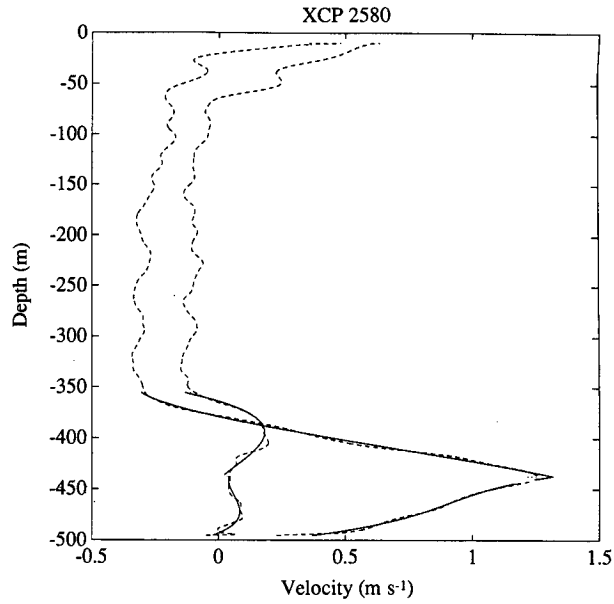

FIG. 3. Both velocity components (dashed lines) from XCP 2580 are fit to two sets of third-order polynomials in the interfacial and bottom layers (solid lines). The fit derivatives are used to obtain the modulus of plume-scale vertical shear of horizontal velocity. The dissipation estimates from the corresponding XDP 1060 (Fig. 2) divided by this modulus result in a profile of the estimated stress on the plume (Fig. 6).

similar pattern is seen in most of the profile pairs. This pattern supports the argument that the two layers are insulated from each other at the nose, with more mixing within each layer than across the nose. The water properties in the plume are consistent with this hypothesis (Fig. 4 of JSB). Water properties in the bottom layer are nearly homogeneous, suggesting vigorous mixing there. In the interfacial layer there are strong linear gradients in water properties, indicating mixing of the plume water with the ambient water above. The change in the vertical gradient of water properties at the nose is further evidence of a barrier to mixing there.

a. Using XDP turbulent dissipation profiles to estimate bottom stress

The law of the wall predicts a mean velocity profile of the form

$$U(z) = \frac{u_*}{\kappa} \ln\left(\frac{z}{z_0}\right) \qquad (1)$$

within the constant stress layer (Tennekes and Lumley 1972). Here $U(z)$ is the mean velocity, $u_* = (\tau/\rho)^{1/2}$ the friction velocity where τ is the constant bottom stress, ρ the density, $\kappa = 0.4$ von Kármán's constant, and z_0 the roughness length. The height above the bottom is z. Owing to the shape of the velocity profile, this portion of the bottom boundary layer is known as the log layer. Within the plume, the turbulent Reynolds

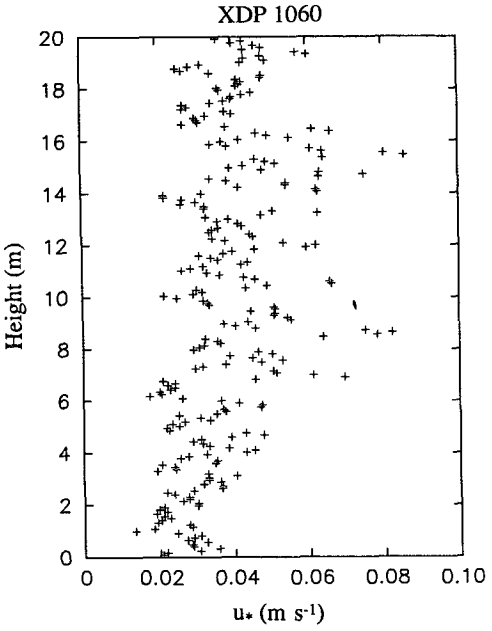

FIG. 4. Friction velocity plotted against height above the bottom for XDP 1060, calculated from (3) using the 0.1-m bin dissipation estimates. The height of the constant stress layer is graphically determined (6 m for XDP 1060). The mean friction velocity below this height is used to determine a stress in the log layer.

stress, $\rho\langle u'w'\rangle$, acting on the mean vertical shear of horizontal velocity, $\partial U/\partial z$, is balanced by the turbulent dissipation, ϵ, and the turbulent buoyancy flux, $g\langle\rho'w'\rangle$, or

$$\rho\langle u'w'\rangle\frac{\partial U}{\partial z} = \epsilon + g\langle\rho'w'\rangle. \qquad (2)$$

The turbulent buoyancy flux should approach zero in the homogeneous bottom boundary layer. Hence, turbulent dissipation is the only term on the right side of (2) within the log layer. Differentiating (1) with respect to z, neglecting turbulent buoyancy flux in (2), and combining the resulting equations, we obtain

$$\epsilon = \frac{\rho u_*^3}{\kappa z}, \qquad (3)$$

where the turbulent Reynolds stress is expressed as the density times the square of the friction velocity, ρu_*^2. This stress is equal to the bottom stress, τ, and is constant within the log layer. By (3), the friction velocity is proportional to the cube root of the turbulent dissipation rate times the height above the bottom.

For each XDP drop, the 0.1-m bin turbulent dissipation estimates are converted to friction velocities using (3). The friction velocities are plotted against height above the bottom (Fig. 4). The height of the constant stress layer is chosen subjectively (by examining each plot) and the mean friction velocity below this height calculated. There are 37 drops yielding high-quality estimates of friction velocity (all symbols except multiply signs; Fig. 1). The standard deviations are around 30% of the means. The means are estimated over heights ranging from 1 to 28 m, with a mean height of 8 m above the bottom, a median of 6 m, and a standard deviation of 5 m. The mean and median heights of the constant stress layer from the dissipation estimates are very similar to those estimated from the velocity profile using XCP data (JSB).

The ratio of the square of the friction velocity estimated from XDP data to the square of the maximum plume velocity, or nose velocity, within the plume from the appropriate XCP is shown in Fig. 5. These quantities are well correlated, showing that the stress on the plume is proportional to its nose velocity squared. Their ratio is about $0.8(\pm0.2)\times10^{-3}$, to within the 95% standard error of the mean, for the 28 probe pairs used (open circles and crosses; Fig. 1). This ratio is about one-third that calculated using the friction velocities estimated from the velocity profiles (cf. Fig. 5 to Fig. 7 of JSB). This discrepancy reflects a difference in the log-layer stress estimates from the two sets of measurements. This difference is addressed in section 4.

b. *Using XCP–XDP pairs to estimate stress profiles*

The data from paired XCP–XDP profiles is used to estimate stress profiles within the plume. As above, it is assumed that the production of turbulent kinetic energy is balanced by turbulent dissipation and turbulent buoyancy flux (2). Outside the homogeneous bottom boundary layer, but still within the plume, the turbulent buoyancy flux is not completely negligible. Oft-quoted work of Osborn (1980) suggests that the turbulent buoyancy flux is limited to a maximum of 0.2 of the turbulent dissipation. In the calculations below, the turbulent buoyancy flux in (2) is completely neglected. Thus dissipation values from the XDPs are divided by

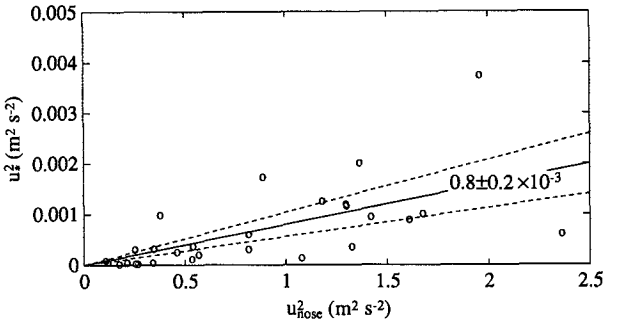

FIG. 5. Squared friction velocities calculated from the dissipation plotted against nose velocities squared. The ratio is $0.8(\pm0.2)\times10^{-3}$ (95% standard error of the mean). Nose velocities are at various distances from the bottom and are not free-stream velocities, being determined by the intersection of bottom and interfacial layers. Compare with Fig. 7 of JSB to see that dissipation-derived stresses are roughly one-third the magnitude of velocity-derived stresses within the log layer.

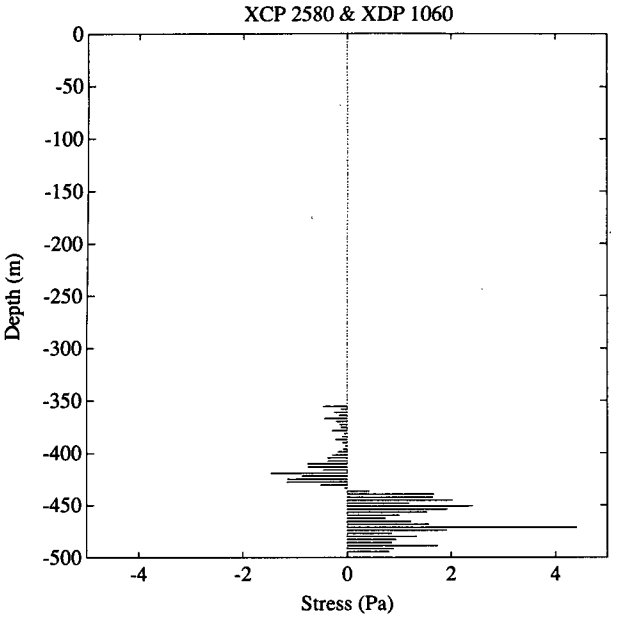

FIG. 6. Profile of stress calculated by dividing 1-s bin estimates of turbulent dissipation from XDP 1060 (Fig. 2) by the plume-scale mean shear of horizontal velocity from XCP 2580 (Fig. 3). Stress estimates within the plume are often on the order of 1 Pa within the interfacial layer and the bottom layer. The bottom-layer means and maxima usually exceed the interfacial layer means and maxima. No typical shape is apparent in the stress profiles.

the vertical shear of horizontal velocity determined from the XCP velocity profiles to obtain stress profiles within the plume.

The 1-s bin turbulent dissipation values from the XDPs are used for this analysis (Fig. 2). Both components of horizontal velocity data from the XCPs are fit to third-order polynomials. Two fits are applied to each profile, one in the bottom layer and one in the interfacial layer. The modulus of plume-scale vertical shear of horizontal velocity at each depth is determined from the derivatives of these fits. This procedure smooths the data such that the plume-scale shear is retained without losing the sharp plume nose (Fig. 3) and reduces the occurrence of locally small moduli of vector shear that produce anomalously large local stress estimates.

Dividing the 1-s bin dissipation values by the plume-scale shear from the polynomial fits results in vertical profiles of stress for each probe pair (Fig. 6). Mean stresses in the bottom and interfacial layers are usually less than 1 Pa each within the plume (Table 1). The individual stress profiles, located throughout the plume (open circles, crosses, and multiply signs; Fig. 1), do not have an obvious typical shape. As will be discussed below, these stress profiles suggest a temporal and spatial variability in the dissipation estimates that may prevent construction of a reliable mean stress profile within the plume with the available data. Note that the XCP and XDP profiles were never closer than 2 min or 200 m in time and space. A mean of many such stress profiles at a single location might be expected to reach a single maximum at the interfacial layer, cross through zero at the plume nose, and then increase toward the bottom, reaching a constant maximum within the log layer.

The mean stress values in the interfacial layer are about 0.4 of those in the bottom layer, with a great deal of variation (Fig. 7). It is the maximum stress values that are dynamically significant. For the hypothetical case of triangular stress profiles within each layer (with a negligibly thick log layer), maximum stresses would be twice the mean values. For parabolic stress profiles this ratio of maximum to mean would be reduced. These ratios could be different for each layer and could vary spatially within the plume. Unfortunately, the maxima cannot be reliably estimated without knowing the shape of the stress profiles, so the more robust means are reported (Table 1). The maxima will always exceed the means. If the ratios of mean to maximum stress are similar in the interfacial and bottom layers, then the interfacial stress contributes only about 0.3 of the total stress on the plume. The scatter in the mean values and their uncertain relation to the maximum stresses make this suggestion tenuous.

The mean stresses for the bottom layer presented in this subsection are well correlated with those estimated for the log layer using only the dissipation measurements (Fig. 8). The ratio of the mean value of stress in the bottom layer to that estimated in the log layer using the dissipation alone in (3) is 0.8 ± 0.2 (95% standard error of the mean). Thus, the mean bottom layer stress is less than that in the log layer, as expected (since the maximum stress in the bottom layer should be in the log layer), but only by a factor of 0.8, just different from one by two standard errors of the mean. The two methods are not entirely independent, since both use the turbulent dissipation data. Nonetheless, these results demonstrate that including vertical shear of horizontal velocity in the estimates gives results consistent with those using dissipation alone, and that

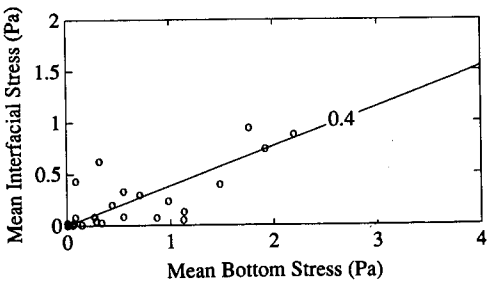

FIG. 7. The mean interfacial stress from the XCP–XDP pairs plotted against the mean bottom stress from the same pairs. The mean ratio of these values, 0.4, suggests that the interfacial stress within the plume is slightly less than the bottom stress. This conclusion is tentative since the relations between the mean stresses and maximum stresses in the two layers are not well known.

TABLE 1. Estimates of mean stresses within the interfacial and bottom layers for XCP–XDP pairs used (open circles, crosses, and asterisks, Fig. 1). The stresses are calculated by dividing the 1-s bin dissipation estimates from each XDP by the plume-scale vertical shear of horizontal velocity at the appropriate depth from the corresponding XCP. The last column is the stress in the log layer estimated from the dissipation profiles alone.

XCP	XDP	$\langle\tau_i\rangle$ (Pa)	$\langle\tau_b\rangle$ (Pa)	ρu_*^2 (Pa)
2538	1034	−0.03	0.07	0.15
2539	1022	−0.02	0.06	0.26
2540	1046	−0.02	0.00	0.05
2541	1043	−0.01	0.14	0.12
2544	704	−0.09	0.27	1.20
2546	1018	−0.01	0.06	0.05
2547	1038	−0.00	0.00	0.07
2548	1039	−0.01	0.01	0.03
2551	813	−0.88	2.20	1.26
2553	806	−0.07	0.87	1.00
2557	1044	−0.01	0.01	0.03
2577	1055	−0.08	0.08	0.26
2578	1072	−0.04	0.06	—
2527	1040	−0.04	0.28	0.26
2530	701	−0.05	1.13	0.54
2530	803	−0.03	0.33	0.33
2523	801	−0.29	0.70	0.99
2528	1035	−0.43	0.08	0.64
2531	709	−0.74	1.92	3.80
2529	808	−0.33	0.55	0.37
2532	707	−0.24	0.98	2.10
2556	1049	−0.14	0.06	—
2556	804	−3.25	8.98	1.10
2580	1060	−0.40	1.48	0.92
2533	807	−0.62	0.31	0.33
2581	1065	−0.13	1.13	1.30
2534	809	−0.20	0.43	0.33
2535	1032	−0.01	0.01	0.02
2536	702	−0.95	1.76	1.80
2579	1059	−0.08	0.55	0.37

the law of the wall and the simple turbulent kinetic energy balance yield similar stress estimates.

4. Discussion

The stresses in the log layer estimated here from dissipation measurements and the velocity profiles (JSB) are both well correlated with the squares of the nose velocities. Both types of estimates have been denoted by ρu_*^2; to avoid confusion we will refer to the dissipation-based estimates as τ_ϵ and those based on the velocity slope as τ_s. By comparing Fig. 5 here with Fig. 7 of JSB one sees that $\tau_\epsilon \approx \tau_s/3$. This discrepancy holds when the estimates from the 24 pairs (open circles and the solid circle; Fig. 1) of profiles are compared directly. A factor of 4.5 was found between stress estimates from turbulent dissipation and velocity data by Dewey and Crawford (1988). They advanced two possible reasons for the discrepancy. First, they noted that their current measurement was taken farther above the bottom than their dissipation data. Thus the current meter may have been outside the region of constant stress. Second, they suggested that form drag may contribute to stress outside the constant stress layer, making the stress calculated from the velocity measurement larger than that estimated from the dissipation data.

In the Gulf of Cadiz experiment, the velocity and dissipation data cover the same range above the bottom. The mean height of the constant stress layer is about 6–8 m as determined by either instrument. The XDP takes data a little closer to the bottom, but the XCP misses only about 10% of the lower end of the constant stress layer. Hence the discrepancy in stress magnitude must arise from something other than differences in sampling range.

At least five effects can cause τ_s to differ from τ_ϵ. (a) Form drag over the rough bottom could be important within the boundary layer, such that τ_ϵ would underestimate the bottom stress. (b) Internal pressure gradients in the plume might cause von Kármán's constant to vary from the value used, affecting the ratios of the two stress estimates as well as their absolute magnitudes, inflating τ_s over τ_ϵ. (c) Partial geostrophic balance in the boundary layer is not taken into account in calculating τ_s, and may also inflate it. (d) Neglecting buoyancy flux within the bottom boundary layer may reduce τ_ϵ, underestimating the bottom stress. (e) Dissipation within the boundary layer may be intermittent, hence possibly undersampled, also causing an underestimate of the stress with τ_ϵ. These five effects are discussed below. Some of these effects adversely impact the use of the log-layer model in determining the stress.

a. Form drag

Form drag may enhance near-bottom shear and stress without affecting the dissipation rate significantly, even close to the bottom. The bottom under the Mediterranean plume is rough. From the Strait of Gibraltar

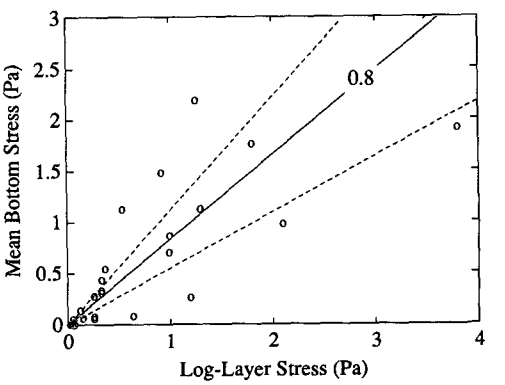

FIG. 8. The stress in the log layer estimated from the 0.1-m bin dissipation data alone plotted against the mean stress of the entire bottom layer calculated from the XDP 1-s bin dissipation values divided by the plume-scale vertical shear of horizontal velocity from the XCP data. The ratio is 0.8 ± 0.2 (95% standard error of the mean), indicating that the mean stress in the bottom layer is less than the stress in the log layer, as expected.

to the edge of the continental shelf the bottom is classified as current swept (Heezen and Johnson 1969) and bottom samples are mostly rock with some sand and gravel. The proportion of gravel and sand increases downstream. There are occasional small, abrupt changes in depth. Sand waves, when present, have amplitudes of 10–20 m with wavelengths of about 200 m. Thus, form drag by objects penetrating into the flow is likely. An extrapolation of the logarithmic velocity profiles (see Fig. 6 of JSB) indicates a virtual bottom at about 0.1 m and flows of 0.2 m s^{-1} within 0.6 m above the bottom.

Form drag produces pressure and velocity anomalies. Vertical divergence of these anomalies is a local sink for turbulent kinetic energy, just like dissipation. A simplified version of the turbulent kinetic energy equation can be written as

$$\left(U\frac{\partial}{\partial x}+W\frac{\partial}{\partial z}\right)\frac{1}{2}\langle q^2\rangle+\tau\frac{\partial U}{\partial z}+\frac{\partial}{\partial z}\left(\langle pw\rangle+\frac{1}{2}\langle q^2w\rangle\right)+\epsilon=0, \quad (4)$$

where $q^2/2$ is the turbulent kinetic energy. This equation balances advection, production, diffusion, and dissipation. The correlation of vertical velocity with either pressure or kinetic energy, the third term of (4), acts to redistribute or diffuse turbulent kinetic energy. The net contribution by this diffusion over the height of the boundary layer is zero, but diffusion can upset the local balance between production and diffusion. This balance is a fundamental assumption in the derivation of (3) and hence τ_ϵ.

Measurements by Antonia and Luxton (1970) in a zero pressure-gradient boundary layer over a rough bottom indicate that dissipation is significantly less than production in the inner 20% of the boundary layer, the ratio being about 2 to 3. The stress and production maxima are not at the wall, but are displaced outward by about 0.15δ, where δ is the boundary-layer thickness. Within 0.2δ of the wall, the dissipation length scale $L_\epsilon = \tau^{3/2}/\epsilon$ and the mixing length scale $l = \tau^{1/2}/(\partial U/\partial z)$ are not equal. However, $l \approx 0.41z$, lending support to the assumption of a logarithmic velocity profile and the use of its slope to estimate the wall stress. The Reynolds number is 3×10^4. A mismatch between production and dissipation in laboratory boundary layers over rough bottoms is observed by Osaka and Mochizuki (1991). They also measure a ratio of 2 to 3 between dissipation and production within 0.2δ of the wall. For the highest Reynolds number reported (5140), the ratio of Reynolds stress to wall stress increases from 0.8 near the wall, to 1 at about 0.15δ, and decreases from there with increasing distance from the wall. In contrast to the results of Antonia and Luxton, both production and dissipation increase toward the wall.

The Reynolds numbers of these laboratory flows are about two to three orders of magnitude smaller than those within the Mediterranean outflow plume. It is not clear to what extent the laboratory measurement for rough walls can be extrapolated to a geophysical flow. Somewhere close to the bottom, diffusion must vanish by virtue of the boundary condition on vertical velocity so dissipation must equal production. There is, however, no a priori reason why the Reynolds stress has to equal the wall stress in such a layer of local balance if pressure forces have a component parallel to the bottom owing to form drag. In laboratory flow, the velocity near the wall collapses to the standard logarithmic profile when normalized by the actual wall stress, and this indicates that τ_s is a more reliable indicator of wall stress than τ_ϵ. It should be noted that in laboratory flows the wall stress is usually measured with force transducers attached to the wall rather than indirectly through velocity measurements as in JSB. If we take the laboratory results at face value, that is, a dissipation rate equal to 2/3 of production and a Reynolds stress equal to 4/5 of the wall stress, then τ_ϵ could be boosted by a factor of $[(3/2)(5/4)]^{2/3} \approx 1.5$ with these corrections.

b. *Internal pressure gradients*

Another reason why τ_s may exceed τ_ϵ is the internal pressure gradient in the Mediterranean outflow plume. Laboratory flows are usually constructed with zero pressure gradient in the boundary layer. Boundary layers below geostrophic flows such as planetary boundary layers may have a downstream pressure gradient owing to entrainment independent of height. In the Mediterranean outflow plume, the pressure gradient is produced by the density anomaly of the plume (Price et al. 1993). Therefore, the gradient varies with height. The gradient is likely to be smallest at the plume top where the plume anomaly approaches the ambient value. The gradient probably increases toward the bottom where the density anomaly is largest. Compared with planetary and laboratory boundary layers, the pressure gradient decreases rapidly downstream owing to mixing and descent to equilibrium depth in the stratified environment.

This difference is significant because the derivation of the law of the wall assumes that there is no pressure gradient and that the turbulence near the wall has only one length scale (distance to the wall) and one velocity scale (the friction velocity u_*). A downstream pressure gradient introduces a second velocity scale

$$u_p = \left(\frac{-\nu}{2\rho}\frac{\partial P}{\partial x}\right)^{1/3} \quad (5)$$

(Tennekes and Lumley 1972), where ν is the viscosity. If the pressure gradient varies with height, the turbulence also has a second length scale. These factors will modify the velocity profile and the relationship between

shear and wall stress. For the case of a favorable and constant pressure gradient without entrainment (a condition that holds for pipes and may be appropriate in limited regions of the Mediterranean outflow plume), von Kármán's constant decreases with increasing Reynolds number to an asymptotic value of 0.33 (Tennekes and Lumley 1972). We are not aware of any work on boundary layers with a height-dependent pressure gradient. Thus, it is possible that von Kármán's constant is significantly different from the value of 0.4 used.

To test how this difference affects the two estimates of stress, we note that

$$\tau_\epsilon = \rho^{1/3}(\epsilon\kappa z)^{2/3} \propto \kappa^{2/3} \tag{6}$$

and

$$\tau_s = \rho\left(\kappa z \frac{\partial U}{\partial z}\right)^2 \propto \kappa^2. \tag{7}$$

Taking the ratio of (6) and (7) gives

$$\frac{\tau_s}{\tau_\epsilon} \propto \kappa^{4/3}. \tag{8}$$

For pipe flow, with the asymptotic value of $\kappa = 0.33$, misuse of the more conventional value of 0.4 would result in a value of τ_s inflated 1.3 times the corresponding value of τ_ϵ. Both values would be overestimates of the actual bottom stress, but τ_s would be inflated more than τ_ϵ.

c. *Geostrophy in the bottom boundary layer*

Stratification coupled with rotation could inflate τ_s with respect to τ_ϵ. Ekman transport produces a cross-stream buoyancy flux. The resulting cross-stream pressure gradient supports the geostrophic reduction of downstream velocity toward the bottom in the bottom boundary layer (MacCready and Rhines 1993). Thus, less stress is required to support a given level of shear. The vertical and horizontal stratification below the nose is small enough that we expect this effect would be small. The CTD station spacing across the sections is not fine enough to estimate horizontal density gradients within the bottom boundary layer, especially with the complicated bathymetry in the region. Crude estimates suggest that the geostrophic shear in the log layer may inflate estimates of τ_s by a factor of as much as 1.3 over τ_ϵ.

d. *Buoyancy flux*

Another mechanism that might cause τ_ϵ to be an underestimate of the bottom stress is the buoyancy flux. This flux, neglected in τ_ϵ, may be larger than the expected maximum value of 0.2 times the turbulent dissipation. This effect is probably not important in the log layer, where density is very nearly homogeneous, but it may be important in the interfacial layer, where water mass properties, as well as mass and volume budgets, suggest that mixing is strong (JSB). Even there, it is unlikely that including this flux could boost stress estimates by a factor of 3, since that would require the turbulent buoyancy flux to be about twice the magnitude of the turbulent dissipation, quite a bit larger than any estimates we are aware of. However, it may play a role in making the dissipation-derived stress estimates obtained smaller than the actual stresses.

e. *Variability*

The last possible explanation of the discrepancy is variability within the bottom boundary layer. Dissipation appears to be intermittent in the Strait of Gibraltar (Wesson 1991). It is possible that it is also intermittent in the Mediterranean outflow plume. The few profiles that show very high values of stress (Table 1) may be an indicator of such intermittence. A relatively small number of dissipation profiles are used to estimate stresses. If dissipation within the plume were intermittent, either temporally or spatially, undersampling would lead to τ_ϵ being an underestimate of the bottom stress. One would need more dissipation data to evaluate this explanation.

5. Conclusions

In JSB, the section-averaged bottom stresses from the XCP velocity profiles are compared with the difference of two bulk budget residuals. A bulk momentum budget estimates the total stresses between section pairs (see also Baringer 1993). Mass and volume transport budget residuals allow estimation of the interfacial stresses between section pairs. The difference of these residuals gives estimates of bottom stresses between section pairs that agree with section-averaged bottom stresses from the XCPs within the error bounds, which are generally close to 1 Pa for estimates near 3 Pa. In the area of high stress on the plume, where the estimates are best, the interfacial stress is close to the bottom stress in magnitude. These patterns are similar to those presented here. However, while the spatial patterns of the stresses are well correlated, the magnitudes of the stresses from the dissipation estimates are smaller than those presented by JSB by about a factor of 3, which is probably a significant difference. The agreement of bulk estimates with local bottom stress estimates from velocity shown in JSB suggests that the local bottom stresses estimated from velocity profiles are closer to the actual mean bottom stresses than those from the dissipation estimates.

Although the dissipation measurements appear to be underestimating the stresses on the plume, further work on this issue is warranted. Section 4 details five possible reasons for the discrepancy, and various combinations of these effects could certainly resolve the

differences between the two sets of estimates. However, the complicated dynamics of the plume make it impossible to sort out which combination is creating the differences. An experiment with dissipation and velocity measured simultaneously within a strong, thick bottom boundary layer over a flat bottom with minimal stratification would help to identify the cause of the discrepancy.

Acknowledgments. This work was supported by the United States Office of Naval Research. Data were collected under Contract N00014-87-K-004 and subsequent analysis was undertaken under Grant N00014-90-J-1100, both to the Applied Physics Laboratory of the University of Washington. More data collection and analysis were performed under Contracts N00014-87-K-0083 and N00014-89-J1707 to The Johns Hopkins University. GCJ was further supported by NOAA's Office of Global Programs. We are indebted to the ship's company and scientific parties on board leg V of R/V *Oceanus* cruise 202 for their assistance in gathering the data. PMEL Contribution Number 1499.

REFERENCES

Antonia, R. A., and R. E. Luxton, 1970: Energy balance in a turbulent boundary layer on a rough wall. *Phys. Fluids,* **14,** 1027–1029.

Baringer, M. O., 1993: Mixing and dynamics of the Mediterranean outflow. Ph.D. thesis, MIT/WHOI, WHOI 93-52, 244 pp.

Dewey, R. K., and W. R. Crawford, 1988: Bottom stress estimates from vertical dissipation rate profiles on the continental shelf. *J. Phys. Oceanogr.,* **18,** 1167–1177.

Heezen, B. C., and G. L. Johnson, 1969: Mediterranean undercurrent and microphysiography west of Gibraltar. *Bull. Inst. Oceanogr. Monaco,* **67,** 1–51.

Johnson, G. C., T. B. Sanford, and M. O. Baringer, 1994: Stress on the Mediterranean outflow plume: Part I. Velocity and water property measurements. *J. Phys. Oceanogr.,* **24,** 2072–2083.

Kennelly, M. A., J. H. Dunlap, T. B. Sanford, E. L. Kunze, M. D. Prater, and R. G. Drever, 1989a: The Gulf of Cadiz expedition: R/V *Oceanus* cruise 202. APL-UW TR 8914, Applied Physics Laboratory, University of Washington, Seattle, WA, 115 pp.

——, M. D. Prater, J. H. Dunlap, E. L. Kunze, and T. B. Sanford, 1989b: XCP data from the Gulf of Cadiz expedition: R/V *Oceanus* cruise 202. APL-UW TR 8925, Applied Physics Laboratory, University of Washington, Seattle, WA, 206 pp.

Lynch, J., and R. Lueck, 1989: Expendable dissipation profiler (XDP) data from the Mediterranean out-flow experiment: R/V *Oceanus* cruise 202 leg V. JHU-CBI TR89-01, The Johns Hopkins University, Chesapeake Bay Institute, Baltimore, MD, 284 pp.

MacCready, P., and P. B. Rhines, 1993: Slippery bottom boundary layers on a slope. *J. Phys. Oceanogr.,* **23,** 5–22.

Osaka, H., and S. Mochizuki, 1991: On the turbulence structure of the boundary layer on a *d*-type rough surface. *Proc. Second World Conf. on Experimental Heat Transfer, Fluid Mechanics, and Thermodynamics,* Dubrovnik, Yugoslavia, 412–423.

Osborn, T. R., 1980: Estimates of the local rate of vertical diffusion from dissipation estimates. *J. Phys. Oceanogr.,* **10,** 83–89.

Prater, M. D., 1991: A method for depth and temperature correction of expendable probes. *J. Atmos. Oceanic Technol.,* **8,** 888–894.

Price, J. F., M. T. O'Neil Baringer, R. G. Lueck, G. C. Johnson, I. Ambar, G. Parrilla, A. Cantos, M. A. Kennelly, and T. B. Sanford, 1993: Mediterranean outflow mixing and dynamics. *Science,* **259,** 1277–1282.

Sanford, T. B., R. G. Drever, J. H. Dunlap, and E. A. D'Asaro, 1982: Design, operation and performance of an expendable temperature and velocity profiler (XTVP). APL-UW TR 8110, Applied Physics Laboratory, University of Washington, 83 pp.

Tennekes, H., and J. H. Lumley, 1972: *First Course in Turbulence.* The MIT Press, 300 pp.

Wesson, J. C., 1991: Turbulence and mixing in the Strait of Gibraltar. Ph.D. dissertation, University of Washington, 316 pp.